

## Measurements of the branching ratio of the $^{209}\text{Bi}(n,\gamma)^{210\text{g}}\text{Bi}/^{210\text{m}}\text{Bi}$ reactions at GELINA

A. Borella<sup>1,2,a</sup>, T. Belgia<sup>3</sup>, E. Berthoumieux<sup>1</sup>, N. Colonna<sup>4</sup>, C. Domingo-Pardo<sup>5</sup>, J.C. Drohe<sup>2</sup>, F. Gunsing<sup>3</sup>, S. Marrone<sup>4</sup>, T. Martinez<sup>6</sup>, C. Massimi<sup>7</sup>, P.M. Mastinu<sup>8</sup>, P.M. Milazzo<sup>9</sup>, P. Schillebeeckx<sup>2</sup>, G. Tagliente<sup>4</sup>, J. Tain<sup>5</sup>, R. Terlizzi<sup>4</sup>, and R. Wynants<sup>2</sup>

<sup>1</sup> CEA/Saclay, DSM/DAPNIA/SPhN, 91911 Gif-sur-Yvette, France

<sup>2</sup> EC-JRC-IRMM, Retieseweg 111, 2440 Geel, Belgium

<sup>3</sup> Institute for Isotopes Hungarian Academy of Sciences, CRC HAS, P.O. Box 77, 1525 Budapest, Hungary

<sup>4</sup> Istituto Nazionale di Fisica Nucleare, Bari, Italy

<sup>5</sup> Instituto de Fisica Corpuscular, CSIC-Universidad de Valencia, Spain

<sup>6</sup> Centro de Investigaciones Energeticas Medioambientales y Tecnologicas, Madrid, Spain

<sup>7</sup> Istituto Nazionale di Fisica Nucleare, Bologna, Italy

<sup>8</sup> Laboratori Nazionali di Legnaro, Legnaro, Italy

<sup>9</sup> Istituto Nazionale di Fisica Nucleare, Trieste, Italy

**Abstract.** Measurements to determine the energy dependent branching ratio for the neutron induced capture reaction on  $^{209}\text{Bi}$  were performed at the time-of-flight facility GELINA of the IRMM in Geel (Belgium). By using germanium  $\gamma$ -ray detectors in combination with the time-of-flight technique, the  $\gamma$ -ray spectra following neutron capture on  $^{209}\text{Bi}$  were determined around 6 neutron resonances between 0.8 keV and 7.0 keV. The relative partial cross sections were obtained by correcting the full energy net peak areas for the effective  $\gamma$ -ray detection efficiency and internal conversion. The effective  $\gamma$ -ray efficiency was obtained from a Monte Carlo model validated through measurements with calibrated sources. The results of a preliminary analysis are given in this paper.

### 1 Introduction

After neutron capture in  $^{209}\text{Bi}$ , the  $\alpha$ -emitter  $^{210}\text{Po}$  ( $T_{1/2} = 138.4\text{d}$ ) is formed due to the  $\beta$ -decay of  $^{210\text{g}}\text{Bi}$  ( $T_{1/2} = 5.013\text{d}$ ). An isomeric state,  $^{210\text{m}}\text{Bi}$  at 271.3 keV, can also be populated and decays by  $\alpha$ -emission with a half-life  $T_{1/2} = 3.04 \times 10^6\text{y}$ . The knowledge of the branching ratio for the  $^{209}\text{Bi}(n,\gamma)^{210\text{g}}\text{Bi}$  and  $^{209}\text{Bi}(n,\gamma)^{210\text{m}}\text{Bi}$  reactions as a function of neutron energy is important for the operation and safety assessment of spallation sources with a liquid lead-bismuth core.

Existing data for the branching ratio are scarce. Recently the  $^{209}\text{Bi}(n,\gamma)^{210\text{m}}\text{Bi}$  and  $^{209}\text{Bi}(n,\gamma)^{210\text{g}}\text{Bi}$  cross sections were measured at thermal energy, first in a pilot experiment at the ILL Grenoble [1], later by a full experiment at the cold neutron beam of the Budapest Neutron Centre and have been reported in refs. [2, 3]. Experimental data at higher energies are reported by Saito et al. [4] at 30 keV and 534 keV.

The existing experimental data indicate that the branching ratio is energy dependent. This hypothesis is enforced by the fact that a large contribution of the feeding of the low-energy levels is due to only few primary  $\gamma$ -ray transitions, which may be subject to fluctuations from one resonance to another. The capture cross section to the ground state  $\sigma_\gamma$  and to the isomeric state  $\sigma_m$  can be determined applying the method proposed by Coceva [5]. By applying this technique,  $\sigma_\gamma$  and  $\sigma_m$  are obtained as the sum of the partial cross sections of  $\gamma$ -rays

feeding these states. For the application of this method it is important to measure the  $\gamma$ -rays emitted after neutron capture with high resolution. In order to study the energy dependence of the branching ratio, an experimental program was set up to cover a wide neutron energy region with neutron time-of-flight measurements.

### 2 Experimental conditions

The measurements were performed at the neutron time-of-flight (TOF) facility GELINA of the Institute for Reference Materials and Measurements (IRMM). The accelerator was operated at 800 Hz and 60  $\mu\text{A}$  average electron current, providing electron pulses of 1 ns width with 100 MeV average electron energy. A detailed description of GELINA can be found in ref. [6].

The measurements were carried out at a 12 m flight path. The angle between the flight path and the direction of the electron beam was 72°. The moderated neutron beam was collimated to about 80 mm in diameter at the sample position. The sample consisted of a disc of 62.214 grams of metallic bismuth with a purity higher than 99.99%, with a diameter of 81.0 mm and a thickness of 1.26 mm, corresponding to  $4.38 \times 10^{-3}\text{at/b}$ . The sample was positioned perpendicularly with respect to the neutron beam.

A  $4.16 \times 10^{-3}\text{at/b}$  thick  $^{10}\text{B}$  anti-overlap filter and a permanent 30 mm thick Pb filter were used to reduce the effect of overlap neutrons and  $\gamma$ -flash, respectively. Using a relatively short flight path length assured a high neutron

<sup>a</sup> Presenting author, e-mail: alessandroborella@yahoo.it

flux and a resolution sufficient to resolve resonances up to 20 keV.

Three high-purity germanium detectors were used. A large volume coaxial detector was used to study the  $\gamma$ -ray spectra up to an energy of 8 MeV and two planar detectors were used to investigate the  $\gamma$ -ray spectrum in the low energy part. The coaxial detector was placed at  $125^\circ$  with respect to the neutron beam, while the two planar detectors were placed at  $55^\circ$  and  $125^\circ$ . This geometry was chosen to minimize systematic effects due to the anisotropy in the  $\gamma$ -ray emission. In order to optimize the experimental conditions, particular care was given to the reduction of the background by using an appropriate lead and boric acid shielding around the measurement area.

In order to reduce the structured background induced by neutron scattering in the sample, the detectors were shielded with  ${}^6\text{LiNH}_2$  and  ${}^6\text{Li}_2\text{CO}_3$  caps together with  ${}^6\text{LiF}$  sheets. Further details about the impact of this so-called neutron sensitivity are given in ref. [7].

After several experiments in different set-ups to optimize the background reduction, the data taking of the final measurement campaign lasted 800 hours of nominal accelerator operation.

### 3 Data analysis

The data, measured with the planar detector positioned at  $125^\circ$  with respect to the neutron beam, were analysed. The linearity and resolution of the detector were monitored weekly by measuring a  ${}^{152}\text{Eu}$  calibration source. In addition, the 139.96 keV  $\gamma$ -ray from the  ${}^{75}\text{Ge}$ , the 511.06 keV annihilation  $\gamma$ -ray and the 870.56 keV  $\gamma$ -ray from  ${}^{17}\text{O}$  were used for an off-line adjustment of the gain using the most recent version of the AGL code [8].

In figure 1 the resulting off-line adjusted spectra of different individual runs are reported. Figure 1 reveals that the data used in the analysis do not suffer from possible instabilities in the recorded detector signal.

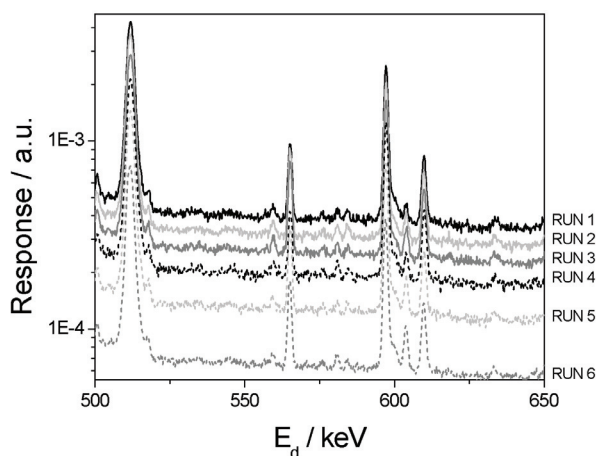


**Fig. 1.** The  $\gamma$ -ray spectra of several runs, after off-line adjustment with the AGL code.  $E_d$  represents the deposited energy in the detector.

The experimental  $\gamma$ -ray spectra up to a deposited energy ( $E_d$ ) of 1.5 MeV were obtained for 6 energy regions around  ${}^{209}\text{Bi}$  neutron resonances at 0.80, 2.32, 3.35, 4.46, 5.11 and 6.53 keV.

The spectra were obtained by selecting a neutron energy region around the resonance. Due to the time resolution and energy spacing of the resonances, some energy regions contained the contribution from more than one resonance. The background of each spectrum was determined by selecting a neutron energy region on the high-energy side of the resonance.

Figure 2 shows the  $\gamma$ -ray spectrum for a neutron energy region around the 0.8 keV resonance. The two intense transitions at 162 keV and 320 keV, feeding the metastable and ground state respectively, can be seen.

In order to obtain the relative intensities of the observed transition, the  $\gamma$ -ray detection efficiency is required. Due to the difference in their strength, each resonance presents a different neutron attenuation and a corresponding  $\gamma$ -ray distribution in the sample. Therefore, the effective detection efficiency, which also accounts for the  $\gamma$ -ray attenuation in the sample, depends on the resonance strength.

The effective  $\gamma$ -ray detection efficiency was deduced with Monte Carlo simulation, using the MCNP code [9]. The detector geometry was carefully modelled and all the shielding materials were accounted for. Figure 3 shows the geometry setup as implemented in the MCNP code. The MCNP model was validated with measurements using a well-characterized  ${}^{152}\text{Eu}$  source. The model efficiency reproduced the measured efficiency within 5%.

In order to determine the distribution of neutron capture along the sample thickness, preliminary MCNP simulations were carried out. The modelled setup is shown in figure 3. The resulting  $\gamma$ -ray emission profiles were used as input for the MCNP simulation to obtain the effective  $\gamma$ -ray detection efficiency.

In figure 4, the resulting effective  $\gamma$ -ray detection efficiencies for the energy region around the 0.8 and

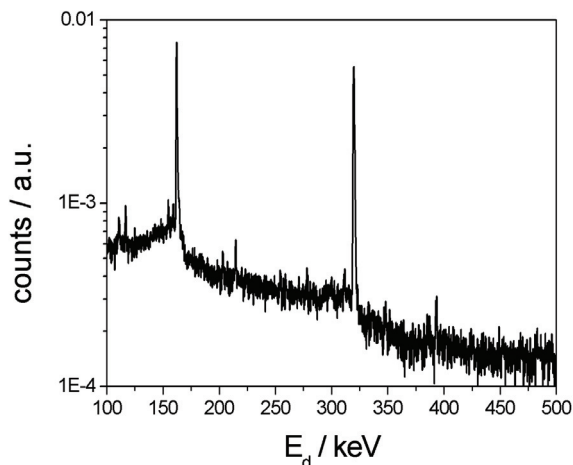


**Fig. 2.** The observed  $\gamma$ -ray spectrum between 100 and 500 keV for a neutron energy around the 0.8 keV neutron resonance.  $E_d$  represents the deposited energy in the detector.

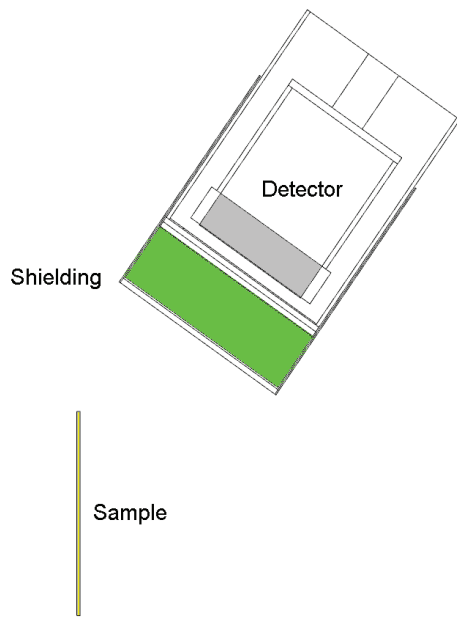


**Fig. 3.** The set-up geometry as modelled in MCNP.

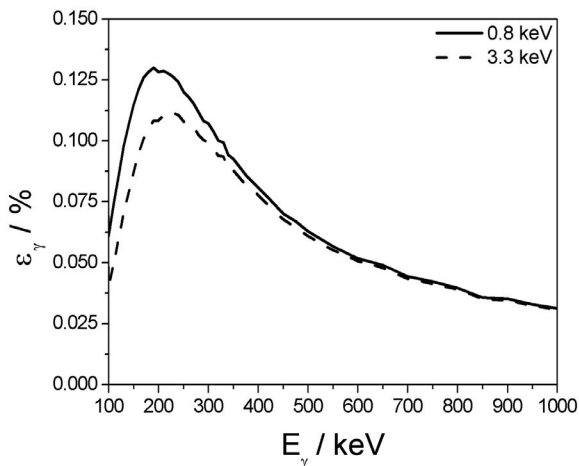


**Fig. 4.** The  $\gamma$ -ray efficiency between 100 and 1000 keV for the energy regions around 0.8 and 3.3 keV.

3.3 keV resonances are shown. The efficiency for the energy region around the 0.8 keV resonance is higher than the efficiency for the energy region around the 3.3 keV resonance. This is due to the different emission profile along the sample thickness. For the energy region around the 0.8 keV resonance, the  $\gamma$ -rays are mainly emitted in the part of the sample which is closer to the detector. Whereas the  $\gamma$ -rays for the weak 3.3 keV p-wave resonance are emitted uniformly across the sample. Therefore, the  $\gamma$ -rays for the 3.3 keV is lower due to a higher effective gamma-ray self absorption.

## 4 Results

To deduce the full energy net peak areas, the  $\gamma$ -ray spectra were analysed with the spectrum analysis program Hypermet-PC [10].

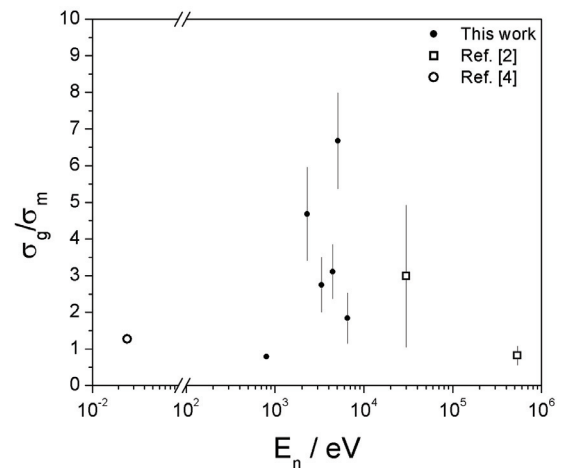


**Fig. 5.** The obtained branching ratio as a function of neutron energy. The results of this work are compared with the results quoted in ref. [2] and ref. [4].

The resulting net peak areas for the observed  $\gamma$ -rays ranging from 0.1 MeV to 1.5 MeV were corrected for the effective  $\gamma$ -ray detection efficiency and for the internal conversion effect. The correction due to internal conversion cannot be neglected, as mentioned in ref. [2]. The branching ratio was obtained by calculating the ratio between the sum of the resulting relative partial cross sections of the transition feeding the ground state and the isomeric state.

The results for 6 energy regions are given in figure 5. The uncertainty results from a 5% uncertainty adopted on the  $\gamma$ -ray efficiency and the uncertainty of the full energy net peak area.

Further data analysis is currently in progress to obtain the branching ratio up to 15.5 keV. In particular the data obtained from the planar detector placed at  $55^\circ$  are important to confirm the quality of the results showed in figure 5. The analysis of the experimental data of the coaxial detector will allow an estimate of the relative intensities for the primary  $\gamma$ -rays of several  $^{209}\text{Bi}$  neutron resonances.

The authors would like to thank Wim Mondelaers and his staff for the skillful operation of the accelerator. We are also grateful to J. Gonzalez for his technical support. This work is supported by the European Commission's 6<sup>th</sup> Framework Programme in the frame of IP-EUROTRANS.

## References

1. A. Letourneau, O. Deruelle, M. Fadil, G. Fioni, F. Gusing, F. Marie, L. Perrot, D. Ridikas, H. Boerner, H. Faust, P. Mutti, G. Simpson, P. Schillebeeckx, *Proc. of 11th International Symposium on Capture Gamma-ray Spectroscopy and Related Topics* (2003), pp. 734–737.
2. A. Borella, G.L. Molnár, T. Belgya, Zs. Révay, L. Szentmiklósi, E. Berthoumieux, F. Gusing, A. Letourneau, F. Marie, *Proc. of the International Conference on Nuclear Data for Science & Technology, ND2004*, pp. 648–651.

3. G.L. Molnár, T. Belgya, Zs. Révay, L. Szentmiklósi, A. Borella, A. Moens, P. Schillebeeckx, R. Van Bijlen, J. Radioanal. Nucl. Chem. **265**(2), 267 (2005).
4. K. Saito, M. Igashira, T. Ohsaki, T. Obara, H. Sekimoto, *Proceedings of the 2002 Symposium on Nuclear Data, November 21-22, JAERI, Tokai, Japan*, pp. 1133–137A.
5. C. Coceva, *Nuovo Cimento, A* **107**, 85 (1994).
6. D. Tronc, J.M. Salomé, K.H. Böckhoff, *Nucl. Instrum. Meth.* **228**, 217 (1985).
7. A. Borella, T. Belgya, E. Berthomieux, N. Colonna, C. Domingo-Pardo, F. Gunsing, S. Marrone, T. Martinez, C. Massimi, P.M. Mastinu, P.M. Milazzo, P. Schillebeeckx, G. Tagliente, J. Tain, R. Terlizzi, R. Wynants, in *Proc. American Nuc. Soc. Topical Meeting on Reactor Physics, Vancouver, Canada, B* **042**, (2006).
8. IRMM, Internal Report (in preparation).
9. J. Briesmeister, *MCNP – A General Monte Carlo N-Particle Transport Code, Version 4C2*, LA-13709-M (2000).
10. B. Fazekas, J. Östör, Z. Kis, A. Simonits, G.L. Molnár, J. Radioanal. Nucl. Chem. **215**, 111 (1997).